Shahid Bahonar University of Kerman

Biomechanism and Bioenergy Research

Online ISSN: 2821-1855
Homepage: https://bbr.uk.ac.ir

Iranian Society of Agricultural Machinery Engineering and Mechanization

Prediction of Pomegranate Seed Oil Oxidation Kinetics under Sunlight Exposure Using Chemometric Modeling

Seyedehsamaneh Shojaeilangari[1], Maryam Manzari Tavakoli[2]✉

[1] Biomedical Engineering Group, Department of Electrical and Information Technology, Iranian Research Organization for Science and Technology (IROST), 33535111, Tehran, Iran
[2] Department of Chemical Technologies, Iranian Research Organization for Science and Technology (IROST), Tehran, Iran
✉ Corresponding author: m.manzaritavakoli69@irost.ir

ARTICLE INFO

Article type:

Research Article

Article history:

Received 07 June 2026

Received in revised form11 July 2026

Accepted 15 August 2026

Available Online 30 September 2026

Keywords:

Pomegranate Seed Oil, Partial Least Squares (PLS), Photo-oxidation, Totox value, Punicic acid

ABSTRACT

Pomegranate seed oil (PSO) is highly valued for its punicic acid content but is extremely susceptible to oxidation, while traditional quality assessment methods are time-consuming and require hazardous chemicals. This study aimed to develop a rapid, non-destructive method for predicting PSO quality using ^{1}H NMR spectroscopy combined with chemometric modeling. Spectra were preprocessed (alignment, normalization, binning at 0.2 ppm into 38 bins). Partial Least Squares (PLS) regression predicted peroxide value (PV), p-anisidine value (p-AV), acid value (AV), and totox value from NMR spectra. The PLS model with one latent variable predicted totox with high accuracy (R^2 = 0.892). Prediction accuracy was also good for p-AV (R^2 = 0.880), AV (R^2 = 0.967), and PV (R^2 = 0.886). Degradation rates showed PV increased rapidly during the first two days (3.73 units/day) then slowed (1.21–1.43 units/day), while p-AV increased at a constant rate (4.84–4.97 units/day). Principal Component Analysis revealed that one component explained 99.6% of total variance, confirming all indices reflect the same oxidative process. The optimal weighting factor for combining PV and p-AV was exactly 2:1, validating the traditional totox formula. This proof-of-concept study demonstrates that ^{1}H NMR spectroscopy combined with PLS regression shows promise as a rapid and non-destructive method for monitoring pomegranate seed oil quality during photo-oxidation. However, further validation with larger, independent datasets is required before routine application in quality control settings.

Cite this article: **Shojaeilangari, S., & Manzari Tavakoli, M. (2026).** Prediction of Pomegranate Seed Oil Oxidation Kinetics under Sunlight Exposure Using Chemometric Modeling. *Biomechanism and Bioenergy Research*, *5* (3), 1-13. https://doi.org/10.22103/bbr.2026.27387.1156

Publisher: Shahid Bahonar University of Kerman
DOI: https://doi.org/10.22103/bbr.2026.27387.1156

INTRODUCTION

Pomegranate has been cultivated for millennia across the Mediterranean region, Middle East, and Iran, where it holds significant cultural and economic importance. While pomegranate juice and arils have received considerable attention for their health benefits, pomegranate seeds are a rich source of valuable oil with unique fatty acid composition. Pomegranate seed oil (PSO) is distinguished by its high content of punicic acid (9-cis, 11-trans, 13-cis octadecatrienoic acid) (Boroushaki et al., 2016), a conjugated linolenic acid isomer that comprises approximately 65–80% of the total fatty acids. Punicic acid has been extensively studied for its potent biological activities, including anti-inflammatory, anti-carcinogenic, anti-atherosclerotic, and antioxidant properties (Carvalho Filho, 2014). Despite these valuable health benefits, the practical application of PSO in food and pharmaceutical industries faces a major challenge: its extreme susceptibility to oxidative deterioration (Manzari Tavakoli et al., 2025). The high degree of unsaturation, particularly the conjugated double bond system of punicic acid, makes PSO highly reactive toward molecular oxygen, light, and heat. Upon exposure to these environmental factors, PSO undergoes rapid auto-oxidation and photo-oxidation, leading to the formation of primary oxidation products (hydroperoxides) and secondary oxidation products (aldehydes, ketones, and other volatile compounds) (Grootveld, 2022). These degradation products not only compromise the nutritional and sensory quality of the oil but also potentially pose health risks to consumers. To ensure product quality and shelf-life, the oxidative status of edible oils is routinely monitored using established chemical indices. The most common quality parameters include: Peroxide Value (PV), which measures primary oxidation products (hydroperoxides); p-Anisidine Value (p-AV), which quantifies secondary oxidation products (aldehydes); Acid Value (AV), which indicates hydrolytic rancidity; and the Totox Value (calculated as 2×PV + p-AV), which provides a comprehensive assessment of overall oxidation state (Zhang et al., 2023). While these methods are reliable and standardized, they suffer from several practical limitations. They are time-consuming, require specialized laboratory equipment and trained personnel, consume hazardous organic solvents, and are destructive to the sample. Furthermore, they provide information only at discrete time points and cannot capture the dynamic, non-linear nature of the oxidation process in real-time (Grootveld, 2022). In recent years, spectroscopic techniques, particularly Proton Nuclear Magnetic Resonance (^{1}H NMR) spectroscopy, have emerged as powerful alternatives for lipid oxidation studies (Hatzakis, 2019). Unlike conventional chemical tests, ^{1}H NMR provides a molecular-level fingerprint of the oil, enabling simultaneous detection and quantification of multiple lipid components, including intact triacylglycerols, free fatty acids, primary and secondary oxidation products, and even isomeric transformations (e.g., cis to trans conversion of double bonds). Moreover, NMR analysis is non-destructive, requires minimal sample preparation, and can be completed within minutes. However, the full potential of ^{1}H NMR for quality prediction is realized only when combined with chemometric techniques, which can extract latent information from complex spectral data (Adade et al., 2025). Among various chemometric methods, Partial Least Squares (PLS) regression has proven particularly effective for spectral data analysis (Wold et al., 2001). PLS is designed to handle datasets with high dimensionality (many spectral variables) and limited sample size, which is typical in kinetic studies of oil oxidation. PLS reduces the dimensionality of the spectral data by projecting it onto a small number of latent variables that ma

MATERIALS AND METHODS

Source of NMR and oxidation data

The ^{1}H NMR spectra and the reference values for PV, p-AV, AV, and Totox value used in this

study were obtained from PSO samples exposed to sunlight for seven days (days 0, 2, 4, and 7), as originally reported in a previous investigation (Manzari Tavakoli et al., 2025). The oxidation parameters were measured according to AOCS official methods, and the raw NMR data are publicly available in the supplementary materials of the same reference.

Nmr Data Preprocessing

For the purpose of this study, the spectra were converted to JCAMP-DX format to enable chemometric modeling. Prior to chemometric modeling, all NMR spectra underwent a series of preprocessing steps to remove irrelevant variations and enhance the quality of the data matrix (Rinnan et al., 2009).

Spectral Alignment

Since slight variations in chemical shift may occur between different samples (due to differences in temperature, pH, or ionic strength), all spectra were aligned to a common reference ppm axis. The Day 0 spectrum (fresh oil) was selected as the reference spectrum because it exhibited the highest signal quality and resolution. The actual recorded NMR data ranged from 0.02 to 7.91 ppm. After removing noisy edge regions and applying binning at 0.2 ppm intervals, the common chemical shift range for analysis was set from 0.22 to 7.62 ppm. Linear interpolation was performed to align each spectrum to the reference ppm axis with a step size corresponding to the original data point spacing.

Baseline Correction and Normalization

To eliminate baseline distortions caused by variations in magnetic susceptibility or improper shimming, an automatic polynomial baseline correction (third-order polynomial) was applied to each spectrum using a modified version of the Bernstein polynomial fitting algorithm (Brown, 1995). After baseline correction, spectral intensities were normalized using total area normalization. In this method, the integrated area of the entire spectrum (from 0.22 to 7.62 ppm) was calculated for each sample, and all intensity values were divided by this total area. Total area normalization compensates for variations in sample concentration and NMR tube positioning, ensuring that only relative changes in spectral patterns are analyzed (Gromski et al., 2015).

Spectral Binning (Bucketing)

To reduce data dimensionality and mitigate the effects of minor peak shifts (which can cause misalignment issues), the continuous NMR spectra were discretized into small, equally spaced intervals called "bins" or "buckets" (Sousa et al., 2013). The optimal bin width was determined by evaluating multiple binning strategies (0.1, 0.2, 0.3, and 0.5 ppm) based on PLS model performance for Totox prediction. While 0.1 ppm preserved higher spectral resolution, it led to lower predictive accuracy likely due to overfitting with the limited number of samples (n=4). Conversely, 0.5 ppm caused excessive information loss. The intermediate bin width of 0.2 ppm provided the best balance between spectral resolution and model stability, achieving the highest predictive accuracy and was therefore selected for all analyses.

Specifically, the spectral range from 0.22 to 7.62 ppm (total width: 7.4 ppm) was divided into 38 bins. The intensity within each bin was calculated as the mean of the original intensity points falling into that interval. This binning procedure reduced the number of predictor variables from approximately 20,000 original data points to 38 bins, which is more suitable for PLS modeling given the limited number of samples (n = 4 time points). The resulting binned spectra were used as the input matrix X (samples × bins) for all subsequent chemometric analyses.

Chemometric Analysis

All chemometric analyses were performed using MATLAB software (version R2023a, MathWorks Inc., Natick, MA, USA) with the Statistics and Machine Learning Toolbox and PLS Toolbox (version 9.0, Eigenvector Research Inc., Wenatchee, WA, USA).

PLS Regression

PLS regression was employed to establish predictive models between NMR spectral data (predictor variables, X) and quality indices

(response variables, Y). PLS is particularly suited for this type of data because it can handle highly collinear predictors (adjacent NMR bins are correlated) and situations where the number of predictor variables (p) exceeds the number of observations (n) (Wold et al., 2001).

For each quality index (PV, p-AV, AV, and Totox), a separate PLS model was constructed. The input matrix X was the binned NMR spectral data (size: 4 samples × 38 bins). The response vector Y was the measured quality index values at the four time points. The PLS algorithm decomposes both X and Y into a small number of latent variables (also called components) that maximize the covariance between X and Y. The general form of the PLS model can be written as:

$$X = T \times P^T + E \quad (1)$$

$$Y = T \times Q^T + F \quad (2)$$

Where T is the score matrix, P and Q are loading matrices for X and Y respectively, and E and F are residual matrices.

Cross-Validation and Model Optimization

To determine the optimal number of latent variables and avoid overfitting, Leave-One-Out Cross-Validation (LOOCV) was performed. In LOOCV, each of the four time points was sequentially left out as a validation set, while the remaining three time points were used as the training set. This process was repeated for each possible number of latent variables (from 1 to 3, the maximum allowed given n = 4). The number of latent variables that produced the lowest Cross-Validated Root Mean Square Error (CV-RMSE) was selected as optimal for each quality index (Westerhuis et al., 2008).

Model Performance Evaluation

The predictive performance of each PLS model was evaluated using the following metrics calculated on the training data (Chicco et al., 2021):

R-squared (R^2): The coefficient of determination, representing the proportion of variance in the response variable explained by the model. R^2 ranges from 0 to 1, with higher values indicating better fit.

$$R^2 = 1 - \frac{\sum_{i=1}^{n}(Y_{actual,i} - Y_{predicted,i})^2}{\sum_{i=1}^{n}(Y_{actual,i} - \bar{Y}_{actual})^2} \quad (3)$$

Root Mean Square Error (RMSE): The standard deviation of the prediction errors. RMSE is expressed in the same units as the response variable.

$$RMSE = \sqrt{\frac{1}{n}\sum_{i=1}^{n}(Y_{actual,i} - Y_{predicted,i})^2} \quad (4)$$

Mean Absolute Error (MAE): The average absolute difference between predicted and actual values.

$$MAE = \frac{1}{n}\sum_{i=1}^{n} |Y_{actual,i} - Y_{predicted,i}| \quad (5)$$

Where n is the number of samples (n = 4).

Additionally, the regression coefficients (beta coefficients) from the final PLS model were examined to identify which spectral regions (ppm bins) contributed most strongly to the prediction of each quality index. Spectral regions with large positive or negative coefficients were interpreted in terms of their chemical significance.

Principal Component Analysis (PCA)

To explore the underlying relationships between the four quality indices, PCA was performed on the quality index data matrix (4 samples × 4 variables). PCA transforms the original correlated variables into a smaller number of uncorrelated Principal Components (PCs) that capture the maximum variance in the data. The first two principal components (PC1 and PC2) were retained for interpretation. The loadings plot was used to identify which quality indices cluster together (indicating strong correlation), while the explained variance ratio indicated how much information each PC captured (Jolliffe & Cadima, 2016).

Determination of Optimal Weighting Factors for Totox

To investigate whether the traditional weighting factor (2 for PV and 1 for p-AV) is optimal for PSO, a separate PLS model was constructed using only PV and p-AV as predictor variables (X = [PV, p-AV]) and Totox as the response variable (Y = Totox). The regression coefficients (beta coefficients) from this model represent the optimal weights for

combining PV and p-AV into a combined index. These coefficients were compared with the traditional weights of 2.00 for PV and 1.00 for p-AV.

Statistical Analysis

All statistical analyses related to the quality indices (PV, p-AV, AV, and Totox) were performed as described in a previously published study (Manzari Tavakoli et al., 2025). Chemometric modeling and preprocessing steps were carried out using MATLAB software (MathWorks Inc., Natick, MA, USA).

RESULTS AND DISCUSSION

Changes in Quality Indices during Photo-Oxidation

Figure 1 shows the evolution of PV, p-AV, AV, and Totox during 7 days of sunlight exposure. The degradation sequence shows normalized values (Day 0 = 1) to compare the relative rate of change across different quality indices. On this normalized scale, the PV (red line) exhibited the steepest slope during the first two days (increasing 3.73-fold), indicating the rapid formation of hydroperoxides during the initial stage of photo-oxidation. In contrast, the Totox value (black line) showed a lower relative increase (2.80-fold) despite having a higher absolute rate of change, because Totox started from a higher baseline value (13.77 vs. 2.73 at day 0). This distinction is important: PV is more sensitive for detecting the onset of oxidation, while Totox provides a better measure of total oxidation products accumulated over time.

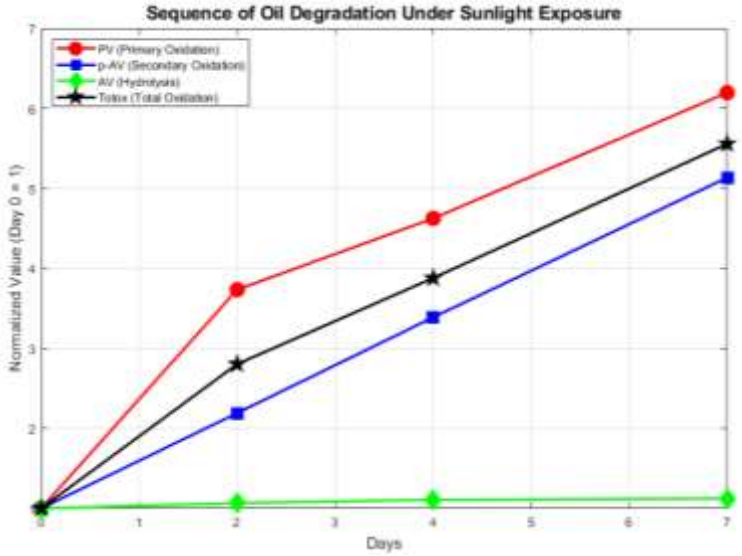

Figure1. Changes in PV, p-AV, AV, and Totox over 7 days

PLS Regression Models for Quality Index Prediction

PLS regression models were developed to predict each quality index (PV, p-AV, AV, and Totox) directly from the binned NMR spectra. LOOCV was used to determine the optimal number of latent variables for each model. The results are summarized in Table 1 and illustrated in Figure 2. The AV model achieved the highest R^2 (0.967), followed by the Totox model (R^2 = 0.892). The PV model showed the lowest R^2 (0.886). The RMSE and MAE followed the same trend.

Table 1. Performance of PLS models for predicting quality indices from NMR spectra

Quality Index	Optimal Components	R-squared (R^2)	RMSE	MAE
PV	1	0.8861	1.7374	1.6306
p-AV	1	0.8797	4.4030	3.5367
AV	1	0.9668	0.0162	0.0154
Totox Value	1	0.8924	7.4756	5.9041

For all four quality indices, the optimal number of latent variables was one (1), indicating that a single latent variable captured most of the covariance between the NMR spectral data and the response variables. This simplicity is advantageous because it reduces the risk of overfitting and improves model interpretability.

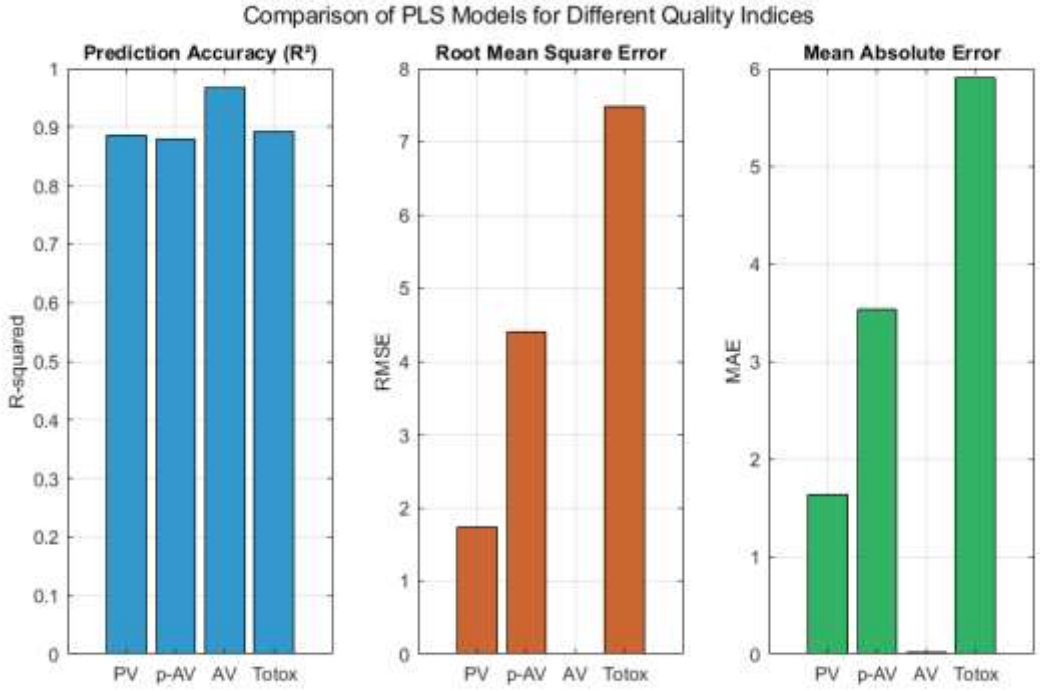

Figure 2. Bar chart comparison of PLS model performance metrics for PV, p-AV, AV, and Totox Valu**e.**

The predictive performance of each PLS model was further evaluated by comparing the predicted values against the actual measured values for all four quality indices. As shown in Figure 3, the predicted values showed good agreement with the measured values, with all points lying close to the identity line (y = x), confirming the good predictive capability of the PLS models.

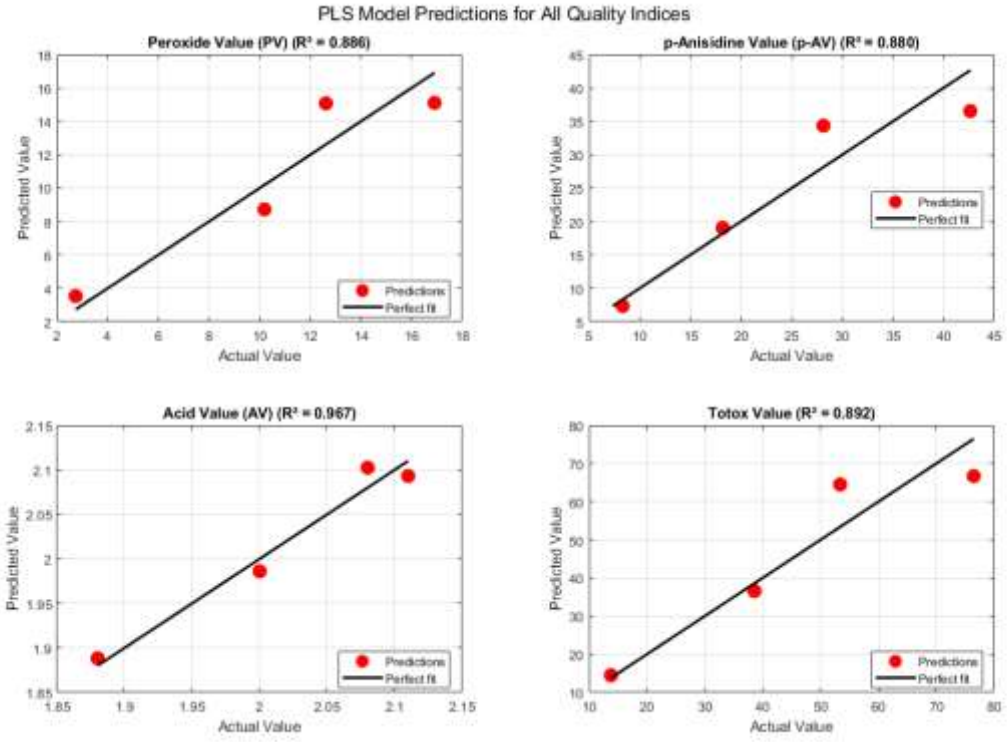

Figure 3. Predicted versus actual values from PLS regression models for (A) PV, (B) p-AV, (C) AV, and (D) Totox Value. R^2 values are shown in each panel. Predictions were obtained using LOOCV with n=4 samples (days 0, 2, 4, and 7).

PLS Regression Coefficients: Identification of Important Spectral Regions

The regression coefficients obtained from the PLS model for Totox value (Figure 4) provide insight into the spectral regions that contribute most strongly to the prediction of oil oxidation status. Spectral variables with negative coefficients indicate regions where signal intensity tends to decrease as oxidation progresses, whereas positive coefficients indicate regions associated with increasing signal intensity and the accumulation of oxidation-related molecular structures. Based on the acquired ^{1}H NMR spectral range (0.22–7.62 ppm after binning), several chemically relevant regions were identified. The olefinic region (5.2–5.8 ppm) exhibited predominantly negative coefficients, suggesting a decrease in unsaturated fatty acid signals during oxidation. This behavior is consistent with the consumption of carbon–carbon double bonds and the degradation of highly unsaturated fatty acids, which are particularly susceptible to oxidative reactions.

The allylic region (2.0–2.2 ppm) showed both positive and negative coefficients, indicating complex chemical transformations during oxidation. This region is associated with allylic protons of conjugated fatty acids in pomegranate seed oil and may reflect simultaneous depletion of native unsaturated lipid structures together with the accumulation of oxidation-derived products and structural rearrangements occurring during storage. Notably, positive coefficients were observed in the 6.0–6.4 ppm region, which is associated with olefinic protons of conjugated fatty acids. The importance of this region is consistent with previous reports describing sunlight-induced cis–trans isomerization of punicic acid to β-

eleostearic acid in pomegranate seed oil (Manzari Tavakoli et al., 2025), resulting in changes in signal intensity within the conjugated olefinic region. These findings demonstrate the capability of ^{1}H NMR spectroscopy to capture structural modifications associated with lipid oxidation and fatty acid isomerization. Characteristic oxidation markers such as aldehydic protons (9–10 ppm) and hydroperoxide-related signals (8.5–9.5 ppm) were outside the acquired spectral window and therefore could not be directly observed in the present dataset.

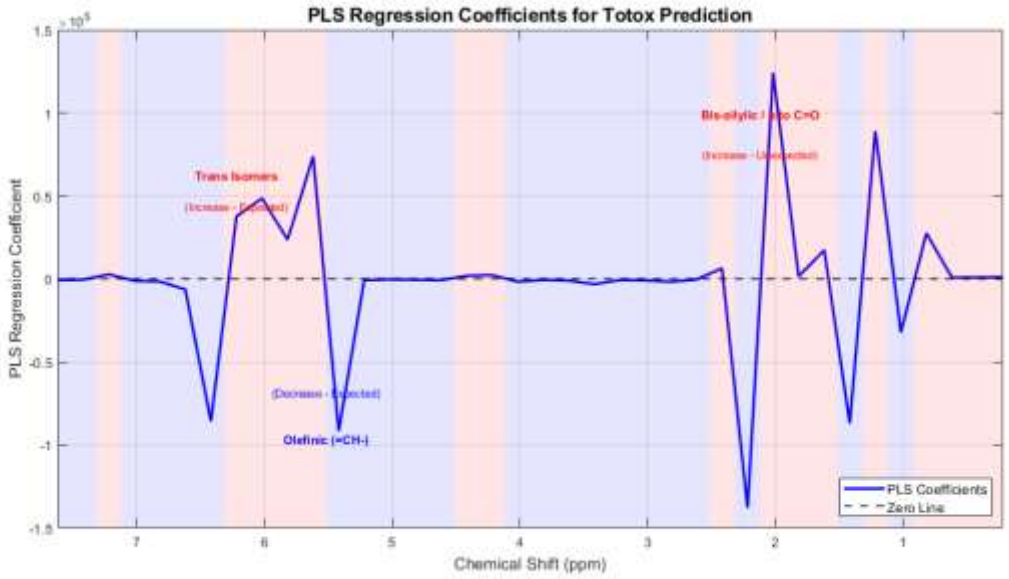

Fi

Figure 4. PLS regression coefficients for Totox prediction from binned ^{1}H NMR spectra (0.2 ppm bins, 0.22–7.62 ppm). Blue shaded regions indicate areas where signal intensity decreases with oxidation. Red shaded regions indicate areas where signal intensity increases with oxidation. The dashed line at zero serves as a reference.

Degradation Kinetics: Primary vs. Secondary Oxidation

The degradation rates calculated from the quality index data are presented in Table 2. The data reveal distinct kinetic behaviors for primary and secondary oxidation.

Table 2. Degradation rates (change per day) during photo-oxidation of PSO under sunlight exposure.

Period	PV Rate (units/day)	p-AV Rate (units/day)	Totox Rate (units/day)
Day 0–2	3.73	4.94	12.40
Day 2–4	1.21	4.97	7.41
Day 4–7	1.43	4.84	7.70

Primary Oxidation (PV): The rate of PV increase was highest during the initial 48 hours (3.73 units/day) and then decreased by approximately 67% to 1.21–1.43 units/day for the remainder of the experiment. This non-linear behavior is consistent with the kinetics of hydroperoxide formation, where the rate is initially high due to the abundance of readily oxidizable unsaturated fatty acids (particularly punicic acid), but then slows as the concentration of these substrates decreases and as natural antioxidant reserves are depleted (E. Choe & D. B. Min, 2006).

Secondary Oxidation (p-AV): In contrast to PV, the rate of p-AV increase remained approximately constant throughout the experiment (4.94, 4.97, and 4.84 units/day for the three periods). This linear behavior indicates

that once the oxidation process is established, secondary oxidation products (aldehydes, ketones, and other carbonyl compounds) are generated at a steady rate that is independent of the declining concentration of primary oxidation products.

Total Oxidation (Totox Value): The Totox rate decreased from 12.40 units/day during days 0–2 to 7.41–7.70 units/day thereafter. This decrease is primarily driven by the slowing of primary oxidation, as secondary oxidation continued at an approximately constant rate throughout the experiment.

PCA of Quality Indices

Principal Component Analysis (PCA) was performed on the quality index data matrix to explore the relationships between the four indices (PV, p-AV, AV, and Totox Value). The results are presented in Table 3.

Table 3. PCA results for quality indices of PSO during photo-oxidation.

Principal Component	Eigenvalue	Variance Explained (%)	Cumulative Variance (%)
PC1	3.98	99.6	99.6
PC2	0.02	0.4	100.0
PC3	<0.01	<0.1	100.0
PC4	<0.01	<0.1	100.0

The first principal component (PC1) alone explained 99.6% of the total variance in the quality index data, indicating that all four indices are highly correlated and essentially reflect a single underlying phenomenon: oxidative deterioration. The second principal component (PC2) explained only 0.4% of the variance, representing minor variations not captured by PC1. The remaining principal components (PC3 and PC4) explained negligible variance (<0.1% each).

The correlation matrix (Figure 5) provides the numerical values of these pairwise relationships.

All pairwise correlations were above 0.93, with the strongest correlations observed between Totox and PV (r = 0.989) and Totox and p-AV (r = 0.993). The high correlation between AV and the other indices (r > 0.94) confirms that even the small changes in free fatty acid content are closely linked to the oxidative degradation process. These findings support the use of Totox as a comprehensive single index for monitoring PSO quality during photo-oxidation.

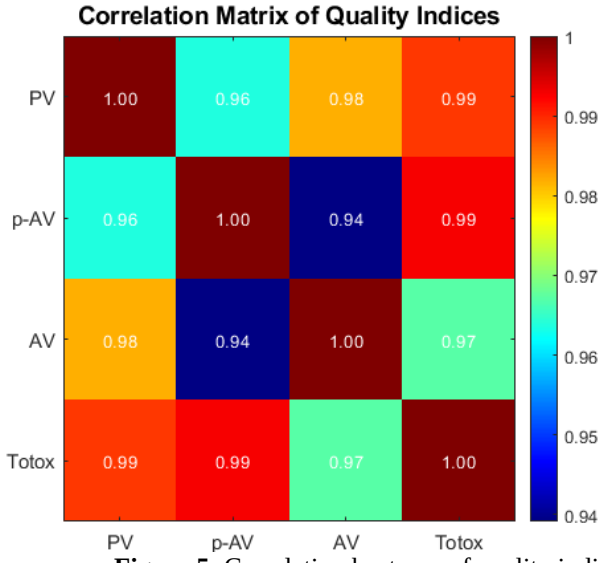

Figure 5. Correlation heatmap of quality indices

Optimal Weighting Factors for Combined Index

To determine whether the traditional weighting factors (2 for PV and 1 for p-AV) are optimal for PSO, a separate PLS model was constructed using only PV and p-AV as predictors of Totox. The regression coefficients from this model represent the optimal weights.

Traditional weighting: Totox = 2.00 × PV + 1.00 × p-AV(6)

PLS-derived optimal weighting: Totox = 2.00 × PV + 1.00 × p-AV (7)

The PLS model yielded weighting factors of 2.00 for PV and 1.00 for p-AV, identical to the traditional formula. The correlation between the traditionally calculated Totox and the reported Totox was 1.0000, as was the correlation between the optimally weighted index and the reported Totox. This finding confirms that the traditional Totox formula (2×PV + p-AV) is appropriate for assessing the total oxidation state of PSO under photo-oxidative conditions.

Comparison of Optimized Regression Methods

To justify the selection of PLS regression, its performance was compared with three alternative methods: Ridge Regression, Principal Component Regression (PCR), and Artificial Neural Networks (ANN). Parameters were optimized for each method to ensure a fair comparison. The results for Totox prediction are summarized in Table 4.

Table 4: Comparison of optimized regression methods for Totox prediction in pomegranate seed oil during photo-oxidation. Methods compared include Partial Least Squares (PLS), Ridge Regression, Principal Component Regression (PCR), and Artificial Neural Network (ANN).

Method	Optimized Parameters	R^2	RMSE
PLS	1 latent variable	0.8924	7.4756
Ridge Regression	$\lambda = 0.1–1000$ (grid search)	Failed	Failed
PCR	3 principal components	-4.8585	0.0000
ANN	1 hidden neuron (Bayesian regularization)	-0.7778	30.3804

Ridge Regression failed despite comprehensive parameter optimization, likely due to the severe imbalance between the limited number of samples (n=4) and the high dimensionality of the spectral data (p=38). PCR showed severe instability with negative R^2, confirming that variance-based dimension reduction is inappropriate for this dataset. ANN severely overfitted even with Bayesian regularization and early stopping, confirming that neural networks require substantially larger datasets (typically hundreds to thousands of samples) for meaningful generalization. PLS demonstrated the best balance of predictive performance and stability, and was therefore selected as the primary modeling method. The interpretability of PLS regression coefficients further supports its use in analytical chemistry applications.

The results of this proof-of-concept study demonstrate that ^{1}H NMR spectroscopy combined with PLS regression shows promise for predicting the quality of pomegranate seed oil during photo-oxidation, achieving R^2 values of 0.886–0.967 for all four quality indices with only a single latent variable. This high predictive performance on the training data, despite having only four time points, indicates that NMR spectra contain sufficient chemical information to correlate with quality indices. However, given the limited dataset, these results should be considered as preliminary evidence rather than conclusive proof that NMR can replace conventional chemical tests. The approach shows promise as a rapid and non-destructive alternative; nevertheless, further validation with larger, independent datasets is required before routine application in quality control settings.

The extreme sensitivity of PSO to photo-oxidation was evident from the rapid increase in PV, which rose nearly 4-fold within the first 48 hours. This behavior is attributed to punicic acid, a conjugated trienoic fatty acid unique to PSO. Unlike non-conjugated polyunsaturated fats, the

conjugated double bond system in punicic acid significantly lowers the bond dissociation energy of bis-allylic hydrogens, making them exceptionally susceptible to hydrogen abstraction by free radicals (Pratt et al., 2011). The non-linear kinetics of PV accumulation, rapid initially then slowing, reflects the classical autoxidation mechanism where hydroperoxides accumulate rapidly during initiation and propagation, then plateau as substrates are depleted and hydroperoxides decompose into secondary products (Zielinski & Pratt, 2017). In contrast, the p-AV increased at an approximately constant rate (4.84 to 4.97 units per day throughout the experiment). This linear behavior is consistent with the classical mechanism of lipid oxidation, where after the initial period, hydroperoxide decomposition proceeds at a faster and relatively constant rate compared to hydrogen abstraction, leading to steady formation of secondary oxidation products such as aldehydes (Schaich, 2020). The AV remained essentially unchanged (1.88 to 2.11 mg KOH/g), confirming that hydrolytic rancidity did not occur under the dry, temperature-controlled conditions. Thus, monitoring PV and p-AV (or Totox alone) is sufficient for quality assessment of PSO during storage (E. Choe & D. B. Min, 2006).

The PLS models achieved the highest accuracy for AV (R^2 = 0.967, RMSE = 0.016), which is remarkable given the minimal absolute change (only 0.23 units over 7 days). This indicates that NMR is sensitive to extremely subtle changes in free fatty acid content, likely because the spectrum captures information from the entire lipid matrix, including changes in molecular mobility and interactions that accompany even minor hydrolysis (Gromski et al., 2015). The slightly lower accuracy for PV (R^2 = 0.886) is expected, as hydroperoxides are transient reactive intermediates whose steady-state concentration represents a dynamic balance between formation and decomposition, introducing variability that a snapshot NMR spectrum cannot fully capture (Farhoosh, 2022).

PCA revealed that a single principal component explained 99.6% of the total variance, confirming that all four quality indices measure the same underlying phenomenon: oxidative deterioration. The high correlations between all indices ($r > 0.93$), particularly between Totox and both PV ($r = 0.989$) and p-AV ($r = 0.993$), support the use of Totox as a comprehensive single index for routine quality control [40]. Furthermore, the PLS-derived optimal weighting factors (2.00 for PV, 1.00 for p-AV) exactly matched the traditional Totox formula, validating its applicability to PSO without modification.

While the results of this proof-of-concept study are encouraging, we acknowledge that the limited sample size (four time points from a single cultivar under one oxidative condition) does not yet justify the replacement of conventional chemical methods in routine quality control. The PLS models developed here require external validation using independent samples with a larger number of time points and a broader range of quality indices before they can be considered robust enough for industrial applications. Therefore, the NMR-based approach should currently be viewed as a complementary tool rather than a complete replacement for conventional chemical testing. Additionally, the potential health implications of trans isomer formation during photo-oxidation warrant further investigation using two-dimensional NMR techniques (Vetica et al., 2020).

Despite these limitations, the high R^2 values on training data and the consistent ranking of model performance provide strong evidence for the feasibility of NMR-based quality prediction. The approach offers several practical advantages over conventional methods: it is non-destructive, requires no hazardous chemicals, provides simultaneous molecular-level information, and can be completed within minutes. However, successful industrial translation will require validation across a broader range of samples, oxidative conditions, and oil matrices.

CONCLUSIONS

This study demonstrated that ^{1}H NMR spectroscopy combined with PLS regression can predict pomegranate seed oil quality during photo-oxidation. PLS models with one latent variable predicted PV (R^2 = 0.886), p-AV (R^2 = 0.880), AV (R^2 = 0.967), and Totox (R^2 = 0.892). Degradation kinetics were non-linear for PV but linear for p-AV, and PCA confirmed all indices reflect the same oxidative process (PC1 = 99.6%). The traditional Totox formula (2×PV + p-AV) was validated as optimal for PSO. The methodology may be extended to other highly unsaturated oils (fish oil, flaxseed oil, walnut oil, perilla oil, echium oil) and adapted for industrial quality control using benchtop low-field NMR systems for in-line monitoring. Future work should validate the models on independent samples, additional cultivars, and more oxidative conditions, and employ 2D NMR techniques for detailed characterization of oxidation products. Successful industrial translation will require validation across broader sample sets and oil matrices.

FUNDING SOURCES

No funding was received for this work

ACKNOWLEDGMENTS

The authors acknowledge the assistance of DeepSeek in the language refinement of this manuscript.

DECLARATION OF COMPETING INTEREST

The authors declare no competing interests

REFERENCES

Adade, S. Y.-S. S., Lin, H., Johnson, N. A. N., Nunekpeku, X., Ekumah, J.-N., Kwadzokpui, B. A., Teye, E., Ahmad, W., & Chen, Q. (2025). Spectroscopic techniques for edible oil evaluation-Technology overview and recent applications from lab to industry. *Food Control*, *176*, 111352. https://doi.org/10.1016/j.foodcont.2025.111352

Boroushaki, M. T., Mollazadeh, H., & Afshari, A. R. (2016). Pomegranate seed oil: A comprehensive review on its therapeutic effects. *Int J Pharm Sci Res*, *7*(2), 430.

Brown, D. E. (1995). Fully automated baseline correction of 1D and 2D NMR spectra using Bernstein polynomials. *Journal of Magnetic Resonance, Series A*, *114*(2), 268–270. https://doi.org/10.1006/jmra.1995.1138

Carvalho Filho, J. M. (2014). Pomegranate seed oil (Punica granatum L.): A source of punicic acid (conjugated α-linolenic acid). *J Human Nutri Food Sci*, *2*(1), 1–11.

Chicco, D., Warrens, M. J., & Jurman, G. (2021). The coefficient of determination R-squared is more informative than SMAPE, MAE, MAPE, MSE and RMSE in regression analysis evaluation. *Peerj computer science*, *7*, e623. https://doi.org/10.7717/peerj-cs.623

Choe, E., & Min, D. B. (2006). Mechanisms and factors for edible oil oxidation. *Comprehensive reviews in food science and food safety*, *5*(4), 169–186. https://doi.org/10.1111/j.1541-4337.2006.00009.x

Farhoosh, R. (2022). New insights into the kinetic and thermodynamic evaluations of lipid peroxidation. *Food chemistry*, *375*, 131659. https://doi.org/10.1016/j.foodchem.2021.131659

Gromski, P. S., Muhamadali, H., Ellis, D. I., Xu, Y., Correa, E., Turner, M. L., & Goodacre, R. (2015). A tutorial review: Metabolomics and partial least squares-discriminant analysis–a marriage of convenience or a shotgun wedding. *Analytica chimica acta*, *879*, 10–23. https://doi.org/10.1016/j.aca.2015.02.012

Grootveld, M. (2022). Evidence-based challenges to the continued recommendation and use of peroxidatively-susceptible polyunsaturated fatty acid-rich culinary oils for high-temperature frying practises: Experimental revelations focused on toxic aldehydic lipid oxidation products. *Frontiers in Nutrition*, *8*, 711640. https://doi.org/10.3389/fnut.2021.711640

Hatzakis, E. (2019). Nuclear magnetic resonance (NMR) spectroscopy in food science: A comprehensive review. *Comprehensive reviews in food science and food safety*, *18*(1), 189–220. https://doi.org/10.1111/1541-4337.12408

Head, T., Giebelhaus, R. T., Nam, S. L., de la Mata, A. P., Harynuk, J. J., & Shipley, P. R. (2024). Discriminating extra virgin olive oils from common edible oils: Comparable performance of PLS-DA models trained on low-field and high-field 1H NMR data. *Phytochemical Analysis*, *35*(5), 1134–1141. https://doi.org/10.1002/pca.3348

Jolliffe, I. T., & Cadima, J. (2016). Principal component analysis: a review and recent developments. *Philosophical transactions. Series A, Mathematical, physical, and engineering sciences*, *374*(2065), 20150202. https://doi.org/10.1098/rsta.2015.0202

Manzari Tavakoli, M., Nikjoo Tavabi, N., Rezadoost, H., Fathi, F., & Nejad Ebrahimi, S. (2025). Comprehensive fatty acids profiling of thirty Iranian pomegranate seed oil cultivars; oil stability and quality through various storage conditions. *Scientific Reports*, *15*(1), 21833. https://doi.org/10.1038/s41598-025-06524-6

Pratt, D. A., Tallman, K. A., & Porter, N. A. (2011a). Free radical oxidation of polyunsaturated lipids: New mechanistic insights and the development of peroxyl radical clocks. *Accounts of chemical research*, *44*(6), 458–467. https://doi.org/10.1021/ar200024c

Pratt, D. A., Tallman, K. A., & Porter, N. A. (2011b). Free radical oxidation of polyunsaturated lipids: New mechanistic insights and the development of peroxyl radical clocks. *Accounts of chemical research*, *44*(6), 458. https://doi.org/10.1021/ar200024c

R**innan, Å., Van Den Berg, F., & Engelsen, S. B. (2009).** Review of the most common pre-processing techniques for near-infrared spectra. *TrAC Trends in Analytical Chemistry*, *28*(10), 1201–1222. https://doi.org/10.1016/j.trac.2009.07.007

Schaich, K. M. (2020). Lipid oxidation: new perspectives on an old reaction. *Bailey's industrial oil and fat products*, *1*, 1-72. https://doi.org/10.1002/047167849X.bio067.pub2

Sousa, S., Magalhaes, A., & Ferreira, M. M. C. (2013). Optimized bucketing for NMR spectra: Three case studies. *Chemometrics and Intelligent Laboratory Systems*, *122*, 93–102. https://doi.org/10.1016/j.chemolab.2013.01.006

Vetica, F., Sansone, A., Meliota, C., Batani, G., Roberti, M., Chatgilialoglu, C., & Ferreri, C. (2020). Free-radical-mediated formation of trans-cardiolipin isomers, analytical approaches for lipidomics and consequences of the structural organization of membranes. *Biomolecules*, *10*(8), 1189. https://doi.org/10.3390/biom10081189

Westerhuis, J. A., Hoefsloot, H. C., Smit, S., Vis, D. J., Smilde, A. K., Van Velzen, E. J., Van Duijnhoven, J. P., & Van Dorsten, F. A. (2008). Assessment of PLSDA cross validation. *Metabolomics*, *4*(1), 81–89. https://doi.org/10.1007/s11306-007-0099-6

Wold, S., Sjöström, M., & Eriksson, L. (2001). PLS-regression: a basic tool of chemometrics. *Chemometrics and Intelligent Laboratory Systems*, *58*(2), 109–130. https://doi.org/10.1016/S0169-7439(01)00155-1

Zhang, Y., Wang, M., Zhang, X., Qu, Z., Gao, Y., Li, Q., & Yu, X. (2023). Mechanism, indexes, methods, challenges, and perspectives of edible oil oxidation analysis. *Critical Reviews in Food Science and Nutrition*, *63*(21), 4901–4915. https://doi.org/10.1080/10408398.2021.2009437

Zhu, M., Shi, T., Luo, X., Tang, L., Liao, H., & Chen, Y. (2020). Determination of the Oxidative Stability of Camellia Oils Using a Chemometrics Tool Based on 1H NMR Spectra and α-Tocopherol Content. *Analytical chemistry*, *92*(1), 932–939. https://doi.org/10.1021/acs.analchem.9b03787

Zielinski, Z. A., & Pratt, D. A. (2017). Lipid peroxidation: kinetics, mechanisms, and products. *The Journal of organic chemistry*, *82*(6), 2817–2825. https://doi.org/10.1021/acs.joc.7b00152